Fast and Accurate Statistical Q-factor computation for impairment-aware RWA problems

Marc Ruiz[1*], Luis Velasco[1], Paolo Monti[2], and Lena Wosinska[2]
[1]Universitat Politècnica de Catalunya (UPC), Barcelona, Spain
[2]Royal Institute of Technology (KTH), Kista, Sweden
*e-mail: mruiz@ac.upc.edu

***Abstract*— Physical layer impairments (PLI) need to be considered in the Routing and Wavelength Assignment (RWA) process in all-optical networks to ensure the provisioning of good quality optical connections (i.e., *lightpaths*). The quality of the provisioned lightpaths can be quantified using the so-called *Q-factor*. Impairment-aware RWA (IA-RWA) algorithms include the *Q-factor* evaluation in their decisions on whether to establish or block new optical connections. Nevertheless, *Q-factor* computation presents some drawbacks that make difficult its use in both online (dynamic) and off-line (static) IA-RWA algorithms. In the case of dynamic scenarios, the long computation times inherent to calculate *Q* values drastically increases lightpath set-up times. On the other hand, the use of *Q-factor* analytical expressions in mathematical programming formulations for static off-line IA-RWA involves those problems to be non-linear, which make them complex and prevents from solving them in practical times. Both, long computation times and non-linearities are mainly as a consequence of *non-linear* impairments computation. In view of that, this paper presents a statistical *Q* model which includes two models to compute Cross Phase Modulation (XPM) noise variance, the dominant non-linear impairment, fitting on-line and off-line IA-RWA scenarios. Exhaustive evaluation reveals that the proposed models provide fast and accurate methods to estimate PLI in terms of *Q-factor* that can be easily used to solve IA-RWA problems.**

***Keywords*: Physical Impairments, *Q*-factor, IA-RWA, Statistical Modeling.**

1 INTRODUCTION

The rapidly increasing traffic demand in communication networks requires further improvement of spectral efficiency in transparent Dense Wavelength Division Multiplexing (DWDM) networks using ever narrower channel spacing and higher bit-rates. In such networks, the signal is transmitted from source to destination through all-optical channels, called lightpaths. With the absence of optical-to-electrical-to-optical (O/E/O) conversions at intermediate nodes, the optical signal might be degraded due to physical layer impairments (PLI) induced by transmission through optical fibers and components. PLI can be divided into *non-linear* and *linear* impairments. Non-linear impairments affect not only each wavelength channel individually, but also cause disturbance and interference among channels traversing the same fiber link. The most important non-linear effects are Self Phase Modulation (SPM), Cross Phase Modulation (XPM), and Four Wave Mixing (FWM). Non-linear impairments become in general apparent as signal power increases in long haul links. On the other hand, linear impairments do not depend on the signal power. The most important linear impairments are fiber attenuation, Amplifier Spontaneous Emission (ASE) noise, Chromatic Dispersion (CD) (or Group Velocity Dispersion (GVD)), and Polarization Mode Dispersion (PMD). PLI of a lightpath can be quantified by using the quality factor Q [1].

To provide good quality lightpaths, PLI information needs to be taken into account while solving the Routing and Wavelength Assignment (RWA) problem. RWA consists in finding a physical route, and in assigning a wavelength to a given connection request. The incorporation of PLI information in the RWA problem for transparent optical networks has recently received a lot of attention, resulting in the development of a number of impairment-aware RWA (*IA-RWA*) algorithms [1]-[7]. IA-RWA algorithms can be either used in the network planning phase when the set of connection requests is known in advance (off-line algorithms) [2], or they can be used to dynamically provision lightpaths at arrivals of connection requests (online algorithms) [3], [4].

Notwithstanding, Q-factor computation adds some drawbacks to the IA-RWA problem and several works in the literature have proposed methods to overcome them (e.g. see [2], [5], [6], [7]). In the case of online IA-RWA algorithms, the main drawback of using Q is the lightpath set-up delay due to the time needed to compute Q. The Q-factor of candidate lightpaths is computed during the lightpath set-up process and only those with a Q-factor above a pre-defined threshold are established. However, before establishing a new lightpath, the Q-factor of already-established lightpaths sharing common links with the new one is re-computed to ensure that their signal qualities will not be degraded below the specified threshold if the new lightpath would be established. As a consequence, all these processes, i.e. collecting lightpaths information and Q-factor re-computation, not only add complexity and control overhead, but also increase lightpath set-up delay. In the case of off-line IA-RWA, computing PLI of lightpaths entails non-linear constraints in mathematical programming formulations to compute non-linear impairments such as FWM or XPM.

Among non-linear impairment XPM is dominant being the value of the XPM variance several times greater than that of FWM. To illustrate this, let us consider a path with a *Q*-factor of 7.3 (Bit Error Rate (BER) ≈ 1.44e-13) the values of variance of XPM and FWM are 1.58e-4 and 5.66e-6 respectively. Thus, in this case, XPM variance is more than 27 times greater than FWM variance. In addition, the computation time needed for calculating the XPM noise variance is several times greater than that for other non-linear effects. In this regard, several works present not only analytical models to compute XPM, but also ways to accelerate that computation. The authors in [8] studied the spectral characteristics of XPM in multi-span optical systems and found that per span dispersion compensation is the most effective way to minimize the XPM effects. In [9] a generalized model of the XPM degradation in fiber links consisting of multiple fiber segments with different characteristics and optical amplifiers is presented. Although this original model was subsequently simplified in other works (e.g.,[10]), *Q*-factor computation times were still in the order of seconds and thus impractical for use in the control plane even using ad-hoc hardware-accelerated computation [11].

Since linear impairment can be pre-computed beforehand, many IA-RWA Integer Linear Programming (ILP) formulations include only linear impairments using pre-computed routes in arc-path formulations [5]. The influence of the wavelength assignment and consequently, of non-linear impairments has been considered in few works such as in [7] where the authors propose an ILP formulation designed for reducing interference between lightpaths as much as possible. They propose to compute the *Q* values of the lightpaths to evaluate its quality in a post-optimization process. However, that method does not take advantage of the *Q* values to improve the solution. Some other works propose ILP formulations with similar constraints combined with iterative methods to compute the *Q* factor during the optimization process. Among them, authors in [2] propose a sophisticated iterative algorithm composed by four simple ILP formulations. The results obtained by these ILPs are afterwards evaluated in terms of *Q* factor and some tuning parameters are modified for the next iteration, until the convergence is reached. In spite of the good quality and performance of this method, the impossibility to embed the *Q* factor computation in the ILP (mainly due to the non-linearity of the XPM mathematical expressions) prevents from reducing the IA-RWA problem with *Q* constraints to a single ILP formulation.

In light of XPM is the dominant non-linear impairment and aiming at significantly reducing its computation times, we propose two novel statistical models to compute lightpaths' XPM noise variance specifically designed to fit dynamic and static scenarios. The first model is based on polynomial fitting. However, since this model is still non-linear we propose a linear approach to estimate XPM. In addition, we assume a worst case for the FWM noise variance, and then its value can be pre-computed beforehand.

The remainder of this paper is organized as follows. Section 2 presents a general description of PLI highlighting some properties of the XPM noise variance. Section 3 designs both the polynomial and the linear XPM models which are validated in section 4 against the exact XPM model currently used. Moreover, since XPM models are part of the statistical *Q* factor computation, exhaustive experiments are performed to validate the *Q* values obtained using our models against values obtained using analytical expressions. Two general applications of our statistical models to solve online and offline IA-RWA problems are described in Section 5. Finally section 6 concludes the paper.

2 IMPAIRMENTS MODEL

This section first presents a description of how the *Q*-factor is computed, then it highlights some interesting properties of XPM variance and subsequent models are presented to take advantage from them.

2.1 Q-factor Computation

As stated in the introduction, the effect of both linear and non-linear PLI can be quantified by using the quality factor *Q*. Authors in [1] considered the *Q*-factor which includes effects of ASE noise, the combined SPM/GVD and optical filtering effects, XPM, and FWM. Here, we extend that model to include also the power penalty due to PMD. ASE, FWM, and XPM are calculated assuming that they follow a Gaussian distribution. The combined SPM/GVD and optical filtering effects are quantified through an eye closure metric calculated on the most degraded bit-pattern. Power penalty due to PMD is calculated based on the length of a lightpath, bit rate and fiber PMD parameter. Based on these assumptions the *Q*-factor of a lightpath is calculated according to the following equation, where $P_{transmitter}$ is the transmitted signal power, pen_{eye} is the relative eye closure penalty attributed to SPM/GVD and optical filtering effects, pen_{PMD} is the power penalty due to PMD, σ^2_{ASE}, σ^2_{XPM}, and σ^2_{FWM} are the electrical variance of ASE noise, XPM, and FWM, respectively. A detailed analytical expression of each term in eq. (1) can be found in [1].

$$Q = \frac{pen_{eye} \cdot P_{transmitter}}{pen_{PMD} \cdot \sqrt{\sigma^2_{ASE} + \sigma^2_{XPM} + \sigma^2_{FWM}}} \tag{1}$$

pen_{eye}, pen_{PMD}, and σ^2_{ASE} can be computed beforehand since their values do not vary with the load of the network (i.e.

currently used wavelength channels). Nonetheless, the values of σ^2_{XPM} and σ^2_{FWM} vary with the load, and they need to be computed for every end-to-end unused wavelength of the candidate route. Due to the fact that σ^2_{XPM} is dominant over σ^2_{FWM}, the *worst case* value of σ^2_{FWM} is assumed in this paper, and thus it can be computed in advance.

2.2 XPM Noise Variance Analysis

Let $G(N, E, W)$ be a graph describing an optical network, where N is the set of nodes, E be the set of fiber links, and W be the ascending frequency ordered set of wavelengths. Every wavelength is associated with an optical channel labeled from 1 to $|W|$. Note that each label uniquely identifies one specific frequency in the spectrum. Additionally, let $\alpha(e)$ be the number of amplifiers in link $e \in E$.

Since the XPM noise variance of a lightpath depends on the physical route and the assigned wavelength, let $\sigma^2_{XPM}(r,\lambda)$ represent the value of XPM variance of a lightpath using route r and wavelength λ. Besides, let $\sigma^2_{XPM}(e,\lambda)$ be the XPM noise variance on reference channel λ in link e. $\sigma^2_{XPM}(e,\lambda)$ represents the interference of every used optical channel in link e over reference channel λ. Equation (2) illustrates the relation between $\sigma^2_{XPM}(r,\lambda)$ and $\sigma^2_{XPM}(e,\lambda)$, where φ_{re} is equal to one if link e in route r.

$$\sigma^2_{XPM}(r,\lambda) = \sum_{e \in E} \varphi_{re} \cdot \sigma^2_{XPM}(e,\lambda) \tag{2}$$

Additionally, let $\sigma^2_{XPM}(e,\lambda,i)$ be the XPM noise variance on reference channel λ as a consequence of channel i, in link e. Aiming at empirically finding some relation between $\sigma^2_{XPM}(e,\lambda)$ and $\sigma^2_{XPM}(e,\lambda,i)$, we developed a classical factorial experiment [12] consisting of thousands of XPM variance computations using the analytical model in [10]. Each computation has been defined by a unique combination of experimental variables, being those the number of link amplifiers, the number of wavelengths, the reference channel, and the state of the other channels (i.e., busy or free). Note that when the number of busy channels is equal to one, the obtained $\sigma^2_{XPM}(e,\lambda)$ value matches with a specific case of $\sigma^2_{XPM}(e,\lambda,i)$. After analyzing the obtained values using statistical correlation tools, the following can be stated without error, where δ_{ei} is equal to 1 if channel i is busy in link e. This is in perfect accordance with similar expressions deduced in [10] and [9].

$$\sigma^2_{XPM}(e,\lambda) = \sum_{\substack{i \in W \\ i \neq \lambda}} \delta_{ei} \cdot \sigma^2_{XPM}(e,\lambda,i) \tag{3}$$

As conclusion, each channel being used by an active lightpath adds some interference to the XPM variance of the reference channel independently of the state of the rest of the channels. This additive behavior paves the way to consider an alternative model to calculate $\sigma^2_{XPM}(e,\lambda)$ based on modeling $\sigma^2_{XPM}(e,\lambda,i)$.

For illustrative purposes, Fig. 1 plots the $\sigma^2_{XPM}(e,\lambda,i)$ values for $i=\lambda+1$ (i.e., interference of the adjacent wavelength channel) and $i= \lambda+2$ (i.e., interference of the wavelength channel at a distance of two with respect to the reference one) with $\lambda=1$ to 79, for links with different values of $\alpha(e)$. As shown, $\sigma^2_{XPM}(e,\lambda,i)$, λ, and $\alpha(e)$ are clearly nonlinearly related. This fact increases the required complexity of the models, since considering simple linear relations among variables leads to models with unacceptable goodness-of-fit.

2.3 Fast XPM Noise Variance Computation

In view of the additive behavior of XPM variance shown above, a very basic approach for modeling $\sigma^2_{XPM}(e,\lambda,i)$ consists of pre-computing and storing the whole set of possible $\sigma^2_{XPM}(e,\lambda,i)$ values (hereafter referred to as *full-deterministic* model). $\sigma^2_{XPM}(e,\lambda,i)$ depends on three discrete variables (i.e. $\alpha(e)$, λ, and i) and then, the set of $\sigma^2_{XPM}(e,\lambda,i)$ values is finite and countable, being its size equal to $|W|*(|W|-1)*maxAmp$, where $maxAmp = max\{\alpha(e), e \in E\}$. Thus, the application of the full-deterministic approach provides an alternative valid method to obtain exact values for the XPM variance. Nevertheless, the weak aspect of this approach is the size of the set of XPM noise variance values to store in real networks. For instance, consider fiber links with a number of amplifiers up to 25 (2,000 km) then the size of the whole set raises to the impractical value of 39,000 for 40, or even to 158,000 for 80 wavelengths.

The size of the set of values to be stored can be decreased at the expense of adding some error. In this regard, recall that although each busy wavelength channel adds some interference to the XPM variance of a certain wavelength reference channel, this interference decreases with the distance between wavelength channels until the gap is too large to produce any significant effect. Then, the first step for reducing the size of the *full-deterministic* model is to determine the range of wavelength channels significantly interfering the reference one. At this point, we define the *channel-interference negligible distance* (η) as the parameter defining the half-size of that range. Thus, those wavelength channels at a distance greater that η from the reference wavelength channel are assumed to have a negligible XPM interference over the reference one. This model is hereafter called *restricted deterministic.*

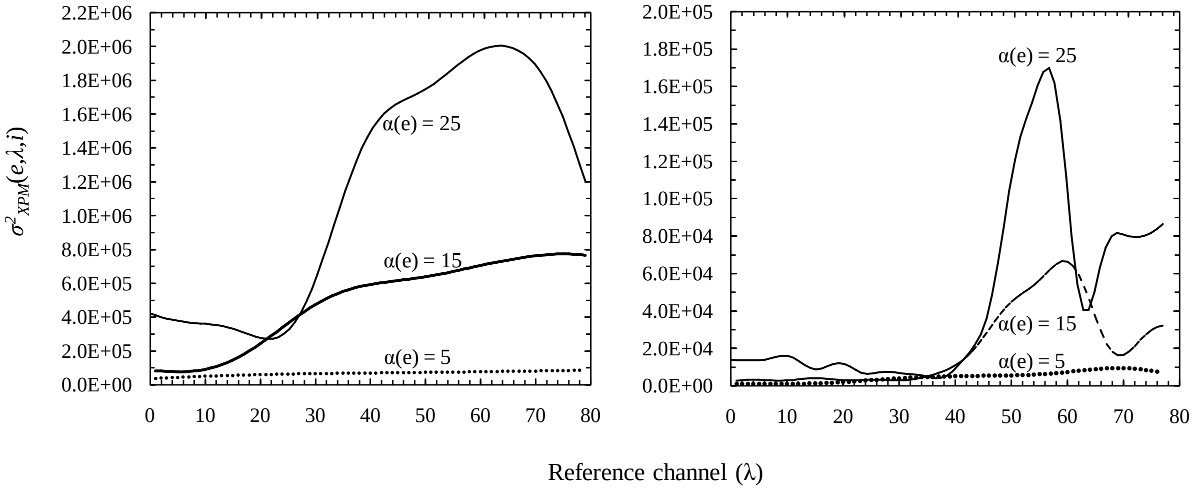

Fig. 1. $\sigma^2_{XPM}(e,\lambda,i)$ plots for $i= \lambda+1$ (left) and $i= \lambda+2$ (right) for links with 5, 15, and 25 amplifiers.

Equation (4) shows the general expression of the restricted deterministic model, where ε_{link} represents the error as a consequence of reducing information, i.e. dismissing every wavelength channels at a distance longer than η. Note that when η=(|W|-1)/2 all wavelengths in the optical spectrum are considered, being the obtained model equal to the full deterministic one (i.e., ε_{link}=0).

$$\sigma^2_{XPM}(e,\lambda) = \sum_{\substack{i=\max(1,\lambda-\eta)\\ i\neq\lambda}}^{\min(\lambda+\eta,|W|)} \delta_i(e)\cdot\sigma^2_{XPM}(e,\lambda,i) + \varepsilon_{link} \tag{4}$$

It is worth noting how, after this first step, the number of $\sigma^2_{XPM}(e,\lambda,i)$ values to be computed in the worst case is reduced to 2η*|W|*$maxAmp$ (from λ-η to λ+η).

Although the size of the restricted deterministic model can be significantly smaller than the one of the full deterministic, it is still too high. For instance, assuming η=4, 16,000 XPM variance values need to be stored when links with 80 wavelengths are considered. Then, aiming at reducing the size of the deterministic models without a significant loss of information, statistical models to accurately compute XPM are proposed in the following section. These models are based on the restricted deterministic one defined in eq. (4).

3 XPM STATISTICAL MODELS

In this section, we propose two different statistical models to predict $\sigma^2_{XPM}(e,\lambda,i)$ with the aim to reduce the size of the deterministic models without introducing significant error.

3.1 The restricted polynomial model

The *restricted polynomial* model consists in finding a polynomial to estimate each $\sigma^2_{XPM}(e,\lambda,i)$ value for those channels in the range [λ-η, λ+η]. We denote that approximate model as $s^2_{XPM}(e,\lambda,i)$, and then $\sigma^2_{XPM}(e,\lambda,i) \approx s^2_{XPM}(e,\lambda,i)$. The mathematical formulation of the polynomial is as follows:

$$s^2_{XPM}(e,\lambda,i) = \sum_{j\in[1,\gamma]} u_{ij}\cdot\lambda^j + \sum_{k\in[1,\gamma]} v_{ik}\cdot\alpha(e)^k + \sum_{j\in[1,\gamma]}\sum_{k\in[1,\gamma]} w_{ijk}\cdot\lambda^j\cdot\alpha(e)^k + b_i \pm \varepsilon_{pair} \tag{5}$$

where u, v, w, and b are the polynomial coefficients. Note that the superscripts on variables indicate the corresponding powers of the polynomial. From eq. (5), the number of coefficients of each $s^2_{XPM}(e,\lambda,i)$ model is (γ^2+2γ+1). Note, however, that some of these coefficients could be zero. Then, the total number of coefficients for the restricted polynomial model (eq. (4) and eq. (5)) is bounded to 2η*(γ^2+2γ+1).

For the sake of simplicity, we have modeled every $s^2_{XPM}(e,\lambda,i)$ with the same parameter γ. The optimal value of γ and the respective polynomial coefficients can be obtained by adapting a classical problem of least squares minimization [12] as follows:

Given:

- a set of σ^2_{XPM} values,

- a η value,
- a target error

Output:

- the degree of the polynomials γ,
- the set of coefficients u, v, w, and b.

Objective: Minimize the degree of the polynomials γ that fits the target error.

The restricted polynomial model opens the possibility to compute XPM variance values from solving a simple mathematical operation. Since the time needed to execute this operation is negligible, the use of this statistical model in online IA-RWA algorithms provides a better performance than the use of recursive XPM variance. Nonetheless, the presence of exponents over λ prevents from using this model in ILP formulations, since the value of λ becomes part of the unknowns of the problem. To overcome this drawback, the next section provides a linear XPM model specially designed to be used in ILP formulations.

3.2 *The restricted linear model*

The restricted linear model for estimating $s^2_{XPM}(e,\lambda,i)$ is a continuous function in λ consisting of a number C of connected linear segments, each represented by a slope and a range of wavelengths. Equation (6) formally states the restricted linear model where f_{eic} and g_{eic} represent the slope and the first wavelength of each segment (*break point*), respectively. Note that the first and last breakpoint are the first and last wavelength in the spectrum, respectively (i.e. $g_{ei1} = 1$ and $g_{eiC+1} = |W|-i$).

$$s^2_{XPM}(e,\lambda,i) = \left\{ f_{eic} \cdot \lambda, \quad \forall g_{eic} \le \lambda \le g_{ei(c+1)} \quad \forall c = 1..C \right\} \tag{6}$$

The coefficients of the restricted linear model are the values of the slopes (f_{eic}) and the break points (g_{eic}). Aiming at reducing the number of coefficients to store, every f_{eic} and g_{eic} can be modeled by means of mathematical expressions such as polynomials, exponential forms, etc. However, λ cannot be part of those expressions to produce a linear function. Therefore, we model f_{eic} following a polynomial of degree ρ using the number of amplifiers in the link as unique variable. Equation (7) illustrates the model to estimate f_{eic}, where t_{icj} represents the j-th coefficient of the polynomial:

$$f_{eic} = \sum_{j \in [0,\rho]} t_{icj} \cdot \alpha(e)^j \tag{7}$$

Regarding g_{eic}, note that it represents an integer in the range 1..|W|. In order to avoid rounding operations and to provide a linear expression, eq (8) defines a linear function that predicts an integer g_{eic} value:

$$g_{eic} = b_{ic} \cdot \alpha(e) + a_{ic} \mid a_{ic}, b_{ic}, g_{eic} \in \mathrm{Z}^+ \tag{8}$$

Note that for each segment we need (ρ+1) coefficients to predict f_{eic} and 2 to predict g_{eic}, being the total size of the restricted linear model $2\eta*(C*(3+\rho))$.

To find the coefficients so to obtain the best goodness-of-fit we face an optimization problem similar to that of the restricted polynomial model. In this case, however, there are two variables to optimize: the number of segments C and the polynomial degree ρ, which can be jointly minimized to reduce the whole size of the model at the expense of increasing the complexity of the optimization problem. For this reason, we divide this problem into two parts: the problem to obtain the optimal value of C; and the problem of fit the optimal value of ρ for the optimal C. For the former, we solve the following optimization problem:

Given:

- a set of σ^2_{XPM} values,
- a η value,
- a target error.

Output

- the number C of segments,
- the set of real coefficients f_{eic} , and integer g_{eic}, a_{ic}, and b_{ic}.

Objective: Minimize C that fits the target error and provides a set of break points that guarantee equation (8).

Once the number of segments is obtained, to problem of finding the minimum size of ρ and its associated t_{icj} values that fit the target error is solved. Since t_{icj} can be fitted with high accuracy by polynomials with relative low degree, the key factor of this restricted linear model is to solve the problem of finding the optimal set of segments with the integrality constraint of the break points estimation.

4 PERFORMANCE EVALUATION

This section first analyzes and compares the performance of each of the XPM models presented above in terms of error and size of the model. The exact $\sigma^2_{XPM}(e,\lambda,i)$ values used for fitting were obtained according to the analytical model in [10]. XPM noise variance values were computed for links with $|W|$=80 and a number of amplifiers ranging from 1 to 25, obtaining 158,000 different values. Next, aiming at providing a final validation of both XPM statistical models, a comparison of the models in terms of the Q value of lightpaths is provided.

4.1 XPM models validation

The models were evaluated in terms of two goodness-of-fit statistics: the Pearson determination coefficient (R^2) and a normalized mean squared error (MSE) [12]. The normalized MSE was obtained by comparing the MSE of a given model against the MSE of the *null model* which contains only one value representing the average of all the $\sigma^2_{XPM}(e,\lambda,i)$. Thus, we compare the error of the models against the error of the more basic (and worst) statistical model where every wavelength of every link produces the same XPM noise regardless of the number of link amplifiers and the frequency in the spectrum. Since the best R^2 possible is 1 (or 100%) and the optimal normalized MSE is 0, we used 1-MSE instead of MSE as goodness-of-fit measure so both statistics can be read in the same way. A normalized 1-MSE value near 90% provides enough precision when the model is used for Q statistical computation, whereas R^2 greater or equal than 95% is enough to validate a model.

Fig. 2 illustrates the impact of the size of η over the amount of information that the restricted deterministic model incorporates. This information, defined as $1-\varepsilon_{link}$, allows measuring the relative effect of the $2*\eta$ neighbor wavelength channels over the XPM value of a certain reference one. Using eq. (4), the amount of information in $\sigma^2_{XPM}(e,\lambda)$ against η is plotted. As shown, the restricted deterministic model with η=4 contains about 97% of information of the full deterministic one, which, as will be proved, is enough for our purposes.

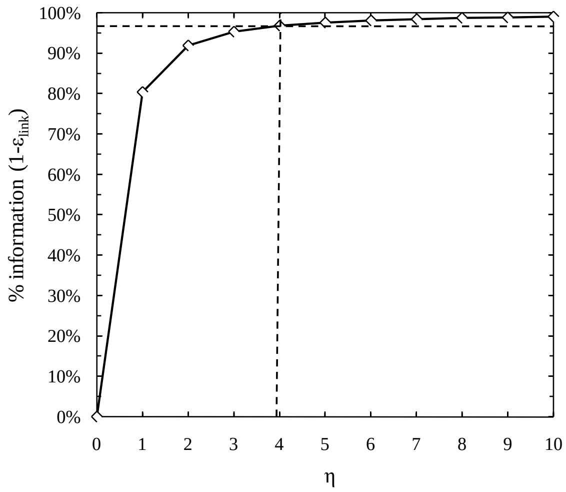

Fig. 2. Amount of information against η

The restricted deterministic with η=4 contains 16,000 coefficients, which ≈10% of the full deterministic size. Since η=4 has been proved to provide a good trade-off between model accuracy and model size, we use that value for the ongoing analysis.

<u>Restricted polynomial</u>

Aiming at obtaining each $s^2_{XPM}(e,\lambda,i)$ in the range of $i=[\lambda-\eta, \lambda+\eta]$, we applied polynomial interpolation to the set of exact $\sigma^2_{XPM}(e,\lambda,i)$ values described in the previous section. As a result of each fit, we obtained a set of polynomial coefficients and the values of the two goodness-of-fit statistics which were used to obtain an overall goodness-of-fit measure of the $\sigma^2_{XPM}(e,\lambda)$ model described in equation (4). Since each wavelength channel in the range defined by η produces a different effect over the reference wavelength channel, the evaluation of the overall goodness-of-fit cannot be done considering a simple summation among the wavelength channels. For this reason, we weighted the goodness of fit of each channel by a measure of the effect that that wavelength channel provides to the XPM of the reference one (obtained from the values depicted in Fig. 2). To this end, we define the weights 0.83, 0.12, 0.03, and 0.02 for $i=\lambda\pm1$, $\lambda\pm2$, $\lambda\pm3$, and $\lambda\pm4$, respectively.

Fig. 3 illustrates the weighted R^2 and normalized 1-MSE for different values of γ. As shown, values close to 95% for

R^2 and 90% for 1-MSE are obtained when degree 5 polynomials are fitted.

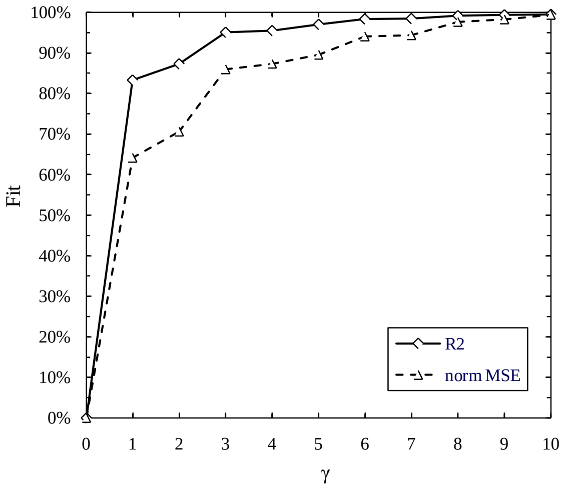

Fig. 3. Fit against γ

Aiming at providing comparison between the restricted polynomial the full-deterministic models with γ=5, we computed $s^2_{XPM}(e,\lambda,i)$ for a set of selected cases. Fig. 4 provides both $\sigma^2_{XPM}(e,\lambda,i)$ exact values (dotted lines) and $s^2_{XPM}(e,\lambda,i)$ fitted ones (solid lines) for $i=\lambda+1$ and $i=\lambda+2$. For the sake of broad comparison we depict three different link sizes in terms of $\alpha(e)$ ranging from 3 to 23. As illustrated, the closer the interference wavelength channel to the reference one, the better is the fitted value. In fact the effect of the first neighboring wavelength channel provides 80% of the total XPM interference over a given reference channel. In light of these results, we conclude that the restricted polynomial model tights the analytical.

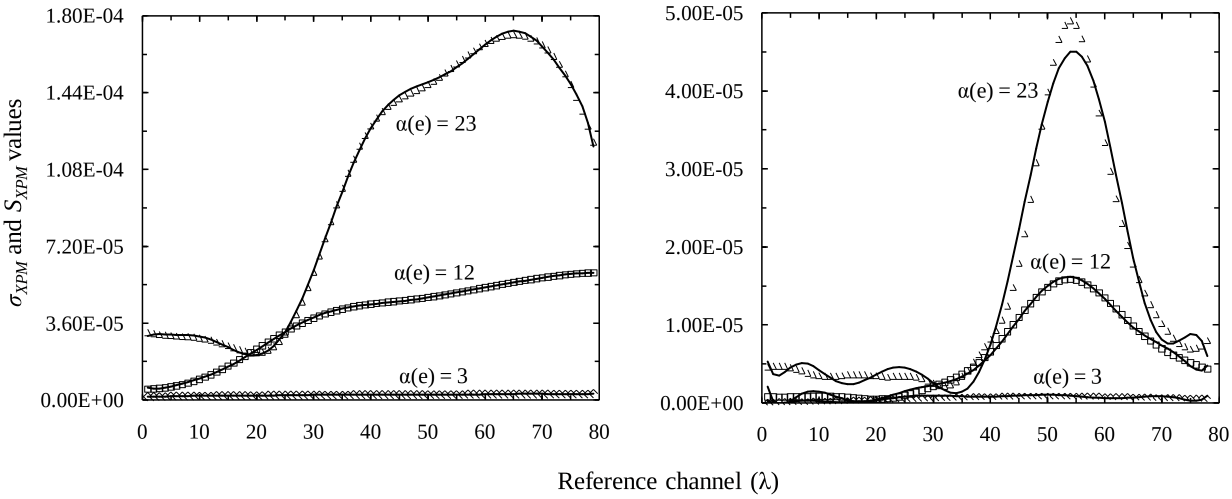

Fig. 4. $\sigma^2_{XPM}(e,\lambda,i)$ and $s^2_{XPM}(e,\lambda,i)$ for $i=\lambda+1$ (left) and $i=\lambda+2$ (right)

To really appreciate the low error introduced by the model, Fig. 5 presents that error as a function of the value of σ^2_{XPM}. A vast majority of values are obtained with an error lower than ±5%. Few of them are computed with higher error but most of those correspond to low σ^2_{XPM} values which add low or negligible total error to the final Q value of a lightpath, as will be proved in the next section. In contrast, error is within ±2.5% for higher σ^2_{XPM} values, those with higher contribution to the final XPM noise variance and Q value of a lightpath.

Finally, regarding the size of the restricted polynomial model, it is worth mentioning that the number of coefficients to be stored falls to 288, in contrast with 39,000 or 158,000 of the deterministic models. Note that this number does not even depend on the considered number of wavelengths in the case of this model. Recall that our model allows predicting the XPM noise variance for links with 80 wavelengths covering a wide range of frequencies.

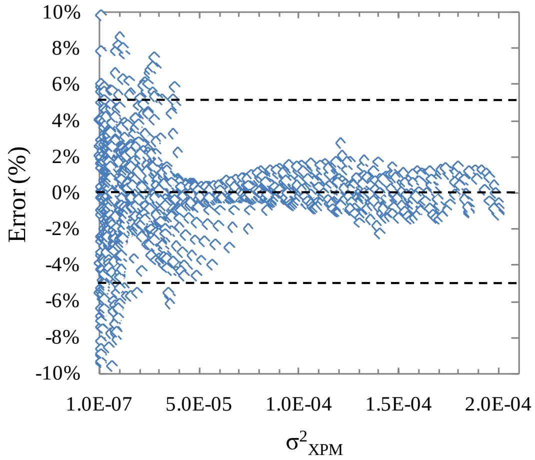

Fig. 5. Restricted polynomial model error

Restricted linear

Similarly to the methodology applied to the restricted polynomial model, we use the weighted R^2 and normalized 1-MSE metrics to compare among different linear models. To solve the problem of finding the optimal number of segments, different sets of break points were generated to ensure the integrality condition in eq. (8) for a given number of segments ranging from 2 to 5. Fig. 6 shows the best obtained value of the goodness-of-fit statistics for each value of C. As shown an good fit is obtained when the number of segments is set to 4. Next, every slope f_{eic} of the optimal set of segments was fitted using the polynomial form described in eq. (7). After testing different values of ρ, we obtain a R^2 greater than 99% for all the slopes when ρ=4.

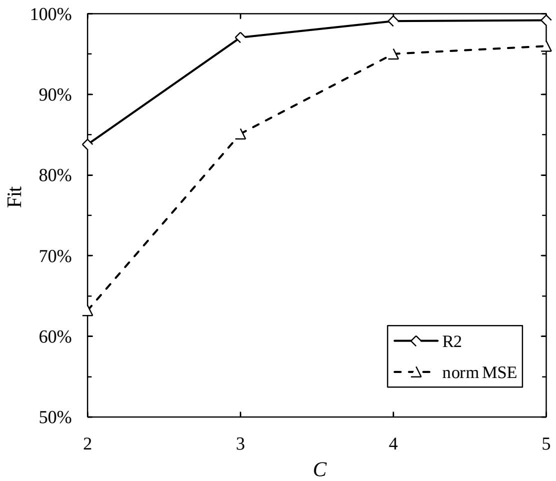

Fig. 6. Fit against the number of segments

Next, prediction of the model using C=4 and ρ=4 was compared against exact values. Similarly to Fig. 4, Fig. 7 shows the predicted $s^2_{XPM}(e,\lambda,i)$ and the exact $\sigma^2_{XPM}(e,\lambda,i)$ values for the same examples used to validate the restricted polynomial model. As observed, the curves of real and fitted values are very close, even when the integrality constraint of the break points restricts the goodness-of-fit of the model. In fact, this condition causes a sub-estimation of the XPM variance when $\sigma^2_{XPM}(e,\lambda,i)$ is high. Similar conclusions can be stated after reviewing the relative error of the restricted linear model shown in Fig. 8. As shown, an error higher than that of the restricted polynomial model can be appreciated clearly trending towards $s^2_{XPM}(e,\lambda,i)$ sub-estimation when the value of $\sigma^2_{XPM}(e,\lambda,i)$ increases. Nevertheless, as proved in the next section, this error does not lead to significant errors in the Q computation.

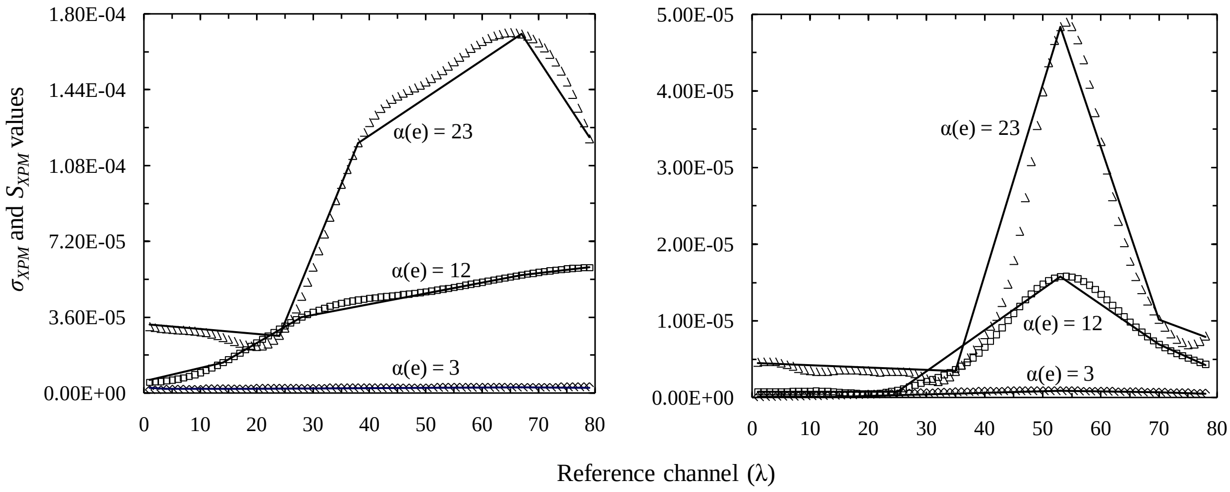

Fig. 7. $\sigma^2_{XPM}(e,\lambda,i)$ and $s^2_{XPM}(e,\lambda,i)$ for i= $\lambda+1$ (left) and i= $\lambda+2$ (right)

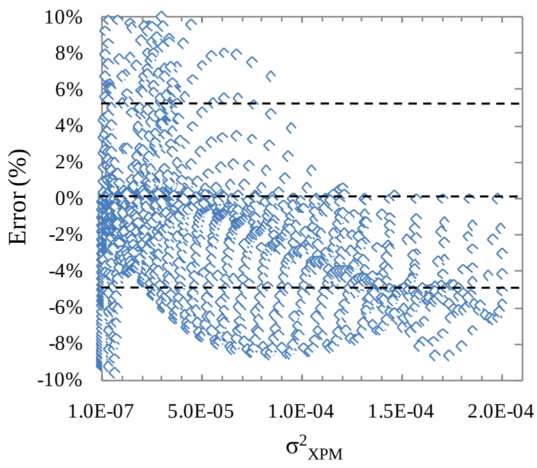

Fig. 8. Restricted linear model error

Regarding the model size, the restricted linear model used in the previous results contains 224 coefficients, which is similar to the size of the restricted polynomial model reducing in 99.8% the size of the full deterministic model.

Table 1 summarizes the number of coefficients and the goodness-of-fit of the described XPM models. The greatest difference among the models is the size of the set of coefficients. On the one hand, the full deterministic model stores the whole set of possible $\sigma^2_{XPM}(e,\lambda,i)$ values (which depends on the number of considered wavelengths per link) and the restricted deterministic reduces that size reducing the amount of information to consider. On the other hand, the size of both the restricted polynomial and the restricted linear model is lower than 1% of the size of the full deterministic model. Regarding the goodness-of-fit, the R^2 of the statistical models is higher than 96%, which represents a tight fit.

4.2 Q-factor statistical computation

In this subsection we compare the *Q* value obtained using one of our two statistical approaches to compute σ^2_{XPM} against the value obtained using the analytical model in [10]. To this end, we randomly generated a set of 15,000 lightpaths each characterized by the number of hops, the length of the links in its route, the assigned wavelength, and the state (busy or free) of the wavelengths channels in each link. We generated each lightpath as a concatenated sequence of links where each link has a random length and load. For each lightpath, we obtained the values of $P_{transmitter}$, pen_{eye}, pen_{PMD}, σ^2_{ASE}, and σ^2_{FWM} from the analytical expressions and reference values detailed in [1]. Besides, three different values for σ^2_{XPM}, one for each model were computed thus obtaining 3 different *Q* values per lightpath.

TABLE 1 XPM MODELS SUMMARY

	|*W*|=40	|*W*|=80	% Information	R^2(%)	1-ECM (100%)
Full deterministic	39,000	158,000	100%	100%	-
Restricted deterministic (η=4)	8,000	16,000	96.85%	100%	-
Restricted polynomial (η=4 γ=5)	288		96.85%	96.93%	89.48%
Restricted linear (η=4, C=4, ρ=4)	224		96.85%	96.14%	92.16%

Fig. 9 compares the *Q* value obtained by the restricted polynomial model against the full deterministic one. Dotted lines represent an error of the 5%, which we considered as the maximum error allowed for statistical *Q* computations. As observed, the *Q* value obtained by the restricted polynomial model tightly fits the exact *Q*.

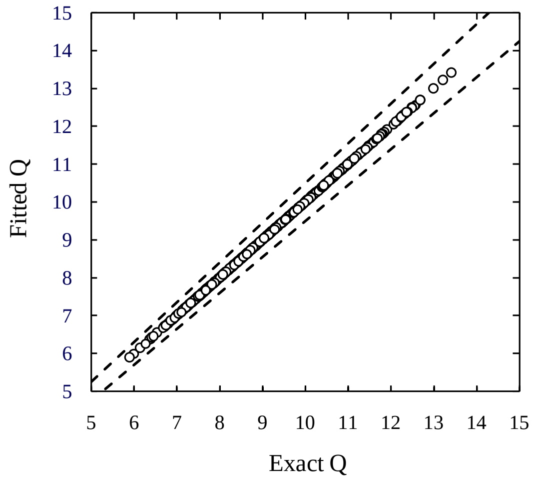

Fig. 9. Exact *Q* against statistical *Q* using the restricted polynomial XPM model

Similarly, Fig. 10 illustrates the goodness-of-fit of the statistical *Q* model when the restricted linear model is used. Although the accuracy of this model is lower than that of the restricted polynomial one, errors are also within the range of 5%. In a deeper analysis, not shown in the figures, we observed than the restricted linear model provides *Q* values slightly higher than the restricted polynomial model. These differences are in line with the relative errors depicted in Fig. 8, where it can be observed that the restricted linear model trends to sub-estimate XPM, thus leading in an over-estimation of *Q* (as can be easily deduced from eq. (1)).

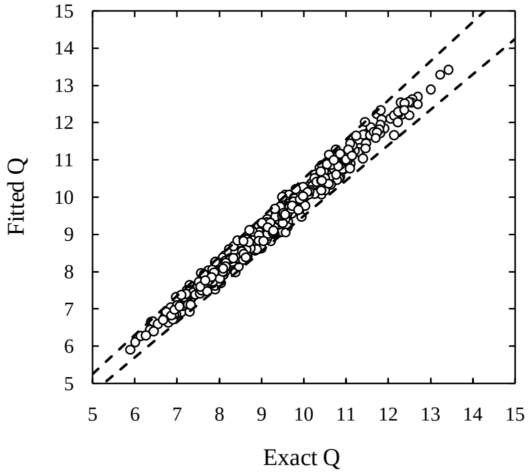

Fig. 10. Exact *Q* against statistical *Q* using the restricted linear XPM model

To weight the impact of the error in the statistical *Q* computation the models were evaluated in terms of wrong decisions to be taken regarding whether the *Q* value of a lightpath is better than a given *Q* threshold. To this end, six different *Q* thresholds (ranging from 7 to 12) were fixed and the amount of lightpaths ensuring each threshold when the *Q* value was computed using the analytical and each statistical model were counted. We define a decision as wrong when the decision taken on a given lightpath using the analytical and a statistical model is different. This is the kind of decisions to be taken when the models are used within IA-RWA algorithms.

Table 2 details the amount of wrong decisions (total and percentage) taken for each model as a function of the *Q* threshold, with respect to the set of 15,000 lightpaths generated. Although the percentage of wrong decisions made by the restricted linear model is significantly higher than the percentage of the restricted polynomial one, the highest error is only 2%, which represents a negligible error in the operation of an IA-RWA algorithm. Note that the quality of service is involved in the case when the connection is accepted by the statistical model being the exact *Q* worse than the threshold. In contrast, the grade of service is involved when the connection is blocked by the statistical model being the exact *Q* better than the threshold. In light of these results, we can conclude that both the restricted polynomial and the restricted linear XPM model provide an accurate statistical *Q* estimation really close to the exact *Q* values.

TABLE 2 STATISTICAL *Q* MODEL VALIDATION

	Q	**7**	**8**	**9**	**10**	**11**	**12**
	# paths	15,000	15,000	15,000	15,000	15,000	15,000
Restricted Polynomial	**Wrong**	13	32	28	20	14	7
	%	0.09%	0.21%	0.19%	0.13%	0.09%	0.05%
Restricted Linear	**Wrong**	137	314	295	257	131	65
	%	0.91%	2.09%	1.97%	1.71%	0.87%	0.43%

To illustrate the usefulness of the *Q* statistical estimation, the next section presents two different application cases in IA-RWA problems, highlighting the advantages of using the proposed models.

5 IA-RWA EXAMPLES

In this section we firstly present a classical online IA-RWA algorithm that takes advantage of the *Q* statistical computation using the restricted polynomial model for estimating the XPM noise variance. Secondly, we define a single ILP formulation for an offline IA-RWA problem that incorporates an accurate *Q* computation by means of the restricted linear XPM model.

5.1 On-line IA-RWA algorithm

In dynamic traffic scenarios the problem of finding a feasible route must be solved each time a connection request arrives. For a route and wavelength assignment to be feasible for an incoming connection request, three conditions must be satisfied: first the involved network resources need to be unused, second, the *Q* factor of the route and wavelength is better than a given threshold, and third, the *Q* factor of all the established lightpaths in the network will remain being higher than the threshold after the new lightpath is established through that route and wavelength. Among different feasible routes and wavelength assignments for a connection request, the one with minimum *Q* value is chosen, i.e. *Q* minimization is the objective function [5]. Then, the online IA-RWA problem can be generically stated as follows:

Given:
- an optical topology G(N, E) where N represents the set of nodes and E the set of fiber links,
- a set of currently established lightpaths L in the optical network,
- a demand d characterized by the source and destination nodes and the required Q threshold.

Output:
- a new lightpath l' for the demand d.

Objective: Minimize the Q of lightpath l'.
Subject to: the Q factor of all the established lightpaths must be higher or equal than the required Q threshold.

Table 3 shows an algorithm to solve the problem stated above. First of all, a set of routes is pre-computed over the topology *G* for the end nodes of the new demand. After finding an available wavelength to establish a route, the *Q* factor is computed for that route. If the route provides a *Q* higher than the threshold, the *Q*-factor is re-computed for all the established lightpaths in order to ensure that the *Q* threshold is still being accomplished. If the demand could be assigned to a route and a wavelength without violating any *Q* threshold, then that route and that wavelength is selected as possible lightpath with a certain *Q* value. Once all the routes and wavelengths are explored and all the possible lightpaths to serve the demand are founded, the one with the highest *Q* value is established. Note that a demand cannot be served when no lightpaths can be established due to lack of resources or *Q* threshold violation.

TABLE 3 ON-LINE IA-RWA ALGORITHM

```
Procedure IA-RWA (IN Node s, d , Lighpath[] lightpaths, OUT, Route r)
begin
    Route[] routes = compute k-ShortestPath (s, d, k)
    Route candidateRoute
    w=0
    bestQ=0

    for each route ri in routes do
        for each wavelength wi in W do
            if wi is end-to-end available in ri then
                thisQ = compute Q-factor using the XPM restricted polynomial model for r and w
                if (thisQ > bestQ) then
                    threshold='true'
                    for each lightpath l in lightpaths do
                        newQ= compute Q-factor using the XPM restricted polynomial model for lightpath l.
                        if newQ<Q_threshold then
                            threshold='false'
                            break for
                    if threshold=='true' then
                        candidateRoute = ri
                        w = wi
                        bestQ = thisQ

    if no candidateRoute found then
        return no route, lack of resources
    if bestQ < Q_threshold then
        return no route, Q reasons
    if threshold=='false'then
        return no route, Q reasons

    return candidateRoute in wavelength w

end
```

As mentioned in the introduction, *Q*-factor computation time can strongly impacts the lightpaths set-up time. This computation time varies depending on the method to compute the XPM noise variance. In this regard, we computed the value of σ^2_{XPM} according to the expressions in [10] for several link distances and wavelength scenarios on a dual-core-based computer with 4 Gbytes of RAM and the computation time was 50ms on average. On the other hand, the time to compute σ^2_{XPM} using the restricted polynomial model is lower than 1 ms, which represents a negligible time. This difference becomes higher when we compare *Q*-factor computation times, which would be in the order of seconds when the exact computation of σ^2_{XPM} is performed (which is in line with [11]), in contrast with few milliseconds needed when the statistical σ^2_{XPM} computation is used.

5.2 Off-line IA-RWA problem

Contrarily to the online IA-RWA problem, in the off-line case all the routes of the demands needed to satisfy the traffic matrix are simultaneously founded over the empty network. Since this problem is an extension of a classical RWA problem, the minimization of the capacity used by the lightpaths can be adopted as the objective function Thus, we define the off-line IA-RWA problem as follows:

Given:

- an optical topology G(N, E) where N represents the set of nodes and E the set of fiber links,
- a set of demands, characterized by the source and destination nodes and the required *Q* threshold.

Output:

- a route and wavelength assignment for each of the demands.

Objective: Minimize the used capacity subject to each demand is routed through a lightpath with a Q higher than the threshold.

As already mentioned, the Q expression in eq. (1) cannot be directly used in an ILP formulation due to its non-linearity. Nevertheless, the elements that only depend on the length of the route, i.e. the linear impairments, can be previously pre-computed if an arc-path [13] formulation is used to define the ILP. This is the case of pen_{PMD} and σ^2_{ASE} that become constant elements, thus being only σ^2_{XPM} and σ^2_{FWM} dependent on the route and wavelength assignment. Since σ^2_{FWM} is several times lower than σ^2_{XPM}, we can assume a worst case for the FWM noise variance ($\sigma^2_{FWM}(WC)$, similarly to [14]), being that a constant value for our problem. At this point, equations (9), (10), and (11) represent a reformulated version of the Q expression in eq. (1) where $A(r)$ and $B(r)$ contain those terms that can be generated as input data of the ILP problem.

$$Q = \frac{A(r)}{\sqrt{B(r) + \sigma^2_{XPM}(r, \lambda)}} \tag{9}$$

$$A(r) = \frac{pen_{eye} \cdot P_{transmitter}}{pen_{PMD}(r)} \tag{10}$$

$$B(r) = \sigma^2_{ASE}(r) + \sigma^2_{FWM}(WC) \tag{11}$$

From equation (9) and given a Q threshold (Q^{thres}), we define the corresponding XPM threshold (XPM^{thres}). More specifically, given a certain route r the maximum amount of XPM noise variance that the lightpath could admit without violating the Q threshold can be defined as follows:

$$XPM^{thres}(r) = \left(\frac{A(r)}{Q^{thres}}\right)^2 - B(r) \tag{12}$$

Therefore, a constraint is added in the RWA ILP that ensures a minimum Q for each lightpath by ensuring a maximum XPM threshold. Using an arc-path formulation and pre-computing the linear impairments and constants, the required Q threshold can be converted into a XPM threshold for each alternative route. Note that the XPM threshold of a demand varies depending on the route due to the linear impairments associated to it. When a route and a wavelength assignment is founded ensuring the required XPM threshold, the required Q threshold is also guaranteed without needing any post-processing computation. Finally, it is worth mentioning that the XPM of each lightpath is computed using the restricted linear model presented in section 3.

The ILP formulation presented below takes advantage from the XPM restricted linear model and the XPM threshold defined in equation (12). For the sake of clarity, we extend the notation of some expressions with the new index d, that represents a specific demand. Then, the following notation is used for sets and parameters:

N	Set of nodes of the network, index n.
E	Set of links of the network, index e.
W	Set of wavelengths, index w.
D	Set of demands, index d.
$R(d)$	Set of routes of demand d, index r.
t_{dre}	Equal to 1 if the route r of the demand d contains the link e.
Q_d^{thres}	Required Q of demand d.
$A(d,r)$, $B(d,r)$	Linear impairments and constants associated to the route r of the demand d.
M	Large positive constant.

The following notation is used for variables:

x_{drw}	Binary, equal to 1 if the demand d is routed following the route r and the wavelength w.
y_{ew}	Binary, equal to 1 if the wavelength channel w is used in the link e.

s_d Real positive, with the statistical XPM variance assigned to demand *d*.

Finally, the ILP formulation is as follows:

$$\min \sum_{e \in E} \sum_{w \in W} y_{ew} \tag{13}$$

subject to:

$$\sum_{r \in R(d)} \sum_{w \in W} x_{drw} = 1, \quad \forall d \in D \tag{14}$$

$$\sum_{d \in D} \sum_{r \in R(d)} t_{dre} \cdot x_{drw} = y_{ew}, \quad \forall e \in E, w \in W \tag{15}$$

$$\sum_{e \in E} t_{dre} \cdot \sum_{\substack{w'=w-\eta \\ w' \neq w}}^{w+\eta} y_{ew'} \cdot s^2_{XPM}(e, w, w') - (1 - x_{drw}) \cdot M \le s_d, \quad \forall d \in D, r \in R(d), w \in W \tag{16}$$

$$s_d \le \sum_{r \in R(d)} \sum_{w \in W} x_{drw} \cdot \left[\left(\frac{A(d,r)}{Q_d^{thres}} \right)^2 - B(d,r) \right], \quad \forall d \in D \tag{17}$$

The objective function (13) minimizes the total amount of used wavelength channels and, thus, the total used capacity. Constraint (14) guarantees that each route is assigned to only one route and wavelength, whereas constraint (15) makes sure that each wavelength channel contains only one lightpath. Constraint (16) computes the XPM noise of each demand according to its route and the occupation of the network using the restricted linear model for $s^2_{XPM}(e,\lambda,i)$ specified in equations (7),(8), and (9). The XPM noise is compared with the threshold permitted by the used route in (17) in order to ensure that all the assigned lightpaths have an XPM noise lower than the threshold and, thus, a *Q*-factor higher that the *Q* threshold.

6 CONCLUSIONS

In this paper, two statistical models to accurately compute the XPM noise variance of lightpaths under both static and dynamic scenarios have been presented. Aiming at reducing the lightpath set-up delay in dynamic scenarios, a polynomial model has been proposed. Although this model allows significantly reducing the *Q*-factor computation time, it cannot be used in classical ILP formulations of the static IA-RWA problem due to its non-linearity. Thus, a linear model has been presented to provide linear expressions to estimate XPM.

Both XPM statistical models were validated against a wide set of values (full deterministic model) obtained from analytical models. The results showed that our models provide a goodness-of-fit greater than 96% in terms of R^2, which represents a high accuracy level. Moreover, the size of both the polynomial and the restricted model remains lower than 288 parameters, thus reducing in more than 99% that of the full deterministic model. Since the main objective of this work is to provide models to estimate lightpaths' *Q*-factor, a final comparison between exact and approximated *Q* values was performed. As proved, the error in terms of *Q* remains lower than the commonly accepted error for statistical models of 5%. Finally, when the *Q* statistical model is used to decide whether or not a path can be established the percentage of wrong decisions remains lower than 2.1%, thus validating the usefulness of the models.

In light of these results, we conclude that the presented statistical models provide a fast and accurate method to estimate the XPM noise variance and, consequently, the *Q*-factor of lightpaths in IA-RWA problems.

REFERENCES

[1] A. Jirattigalachote, P. Monti, L. Wosinska, K. Katrinis, A. Tzanakaki, “ICBR-Diff: an Impairment Constraint Based Routing Strategy with Quality of Signal Differentiation,” Academy Publisher J. of Netw., vol. 5, pp. 1279-1289, 2010.

[2] P. Pavon-Mariño, et al., "Offline Impairment Aware RWA Algorithms for Cross-Layer Planning of Optical Networks," IEEE/OSA J. Lightwave Technol., vol. 27, pp. 1763-1775, 2009.

[3] R. Martínez, et al., "Challenges and Requirements for Introducing Impairment-Awareness into the Management and Control Planes of ASON/GMPLS WDM Networks," IEEE Communications Magazine, vol. 44, pp. 76-85, 2006.

[4] F. Agraz, et al., "Experimental Demonstration of Centralized and Distributed Impairment-Aware Control Plane Schemes for Dynamic Transparent Optical Networks," IEEE/OSA Optical Fiber Communication Conference (OFC), 2010.

[5] S. Azodolmolky, M. Klinkowski, E. Marín, D. Careglio, J. Solé-Pareta, and I. Tomkos, "A Survey on Physical Layer Impairments Aware Routing and Wavelength Assignment Algorithms in Optical Networks," Elsevier Computer Networks, vol. 53, pp. 926-944, 2009.

[6] D. Monoyios and K. Vlachos, "Multiobjective Genetic Algorithms for Solving the Impairment-Aware Routing and Wavelength Assignment Problem," IEEE/OSA J. Opt. Commun. Netw., vol. 3, pp. 40–47, 2011.

[7] K. Manousakis, K. Christodoulopoulos, and E. A. Varvarigos, "Impairment-Aware Offline RWA for Transparent Optical Networks," in Proc. of INFOCOM 2009, pp.1557~1565.

[8] R. Hui, K. Demarest, and C. Allen, "Cross-Phase Modulation in Multispan WDM Optical Fiber Systems," IEEE/OSA J. Lightwave Technol., vol. 17, pp. 1018-1026, 1999.

[9] A. Cartaxo, "Cross-Phase Modulation in Intensity Modulation-Direct Detection WDM Systems with Multiple Optical Amplifiers and Dispersion Compensators," IEEE/OSA Journal of Lightwave Technology, vol.17, pp.178-190, 1999.

[10] S. Pachnicke and E. Voges, "Analytical assessment of the *Q*-factor due to cross-phase modulation (XPM) in multispan WDM transmission systems," in Proc. SPIE, 2003.

[11] Y. Qin, et al. "Demonstration of C/S based Hardware Accelerated QoT Estimation Tool in Dynamic Impairment-Aware Optical Network," in Proc. European Conference on Optical Communication (ECOC), 2010.

[12] D. Montgomery, "Design and Analysis of Experiments," Wiley & Sons, 2004.

[13] M. Pióro and D. Medhi, *Routing, Flow, and Capacity Design in Communication and Computer Networks*, Elsevier, 2004.

[14] S. Pachnicke, T. Paschenda, and P. Krummrich, "Assessment of a constraint-based routing algorithm for translucent 10 Gbits/ s DWDM networks considering fiber non-linearities," OSA J. of Opt. Netw., vol. 7, pp. 365-377, 2008.